Chemical Engineering Journal 164 (2010) 10–15

Contents lists available at ScienceDirect

Chemical Engineering Journal

journal homepage: www.elsevier.com/locate/cej

Marangoni effect in a falling film microreactor

Paweł Sobieszuk[a,*], Ryszard Pohorecki[a], Paweł Cygański[a], Manfred Kraut[b], Frank Olschewski[c]

[a] Faculty of Chemical and Process Engineering, Warsaw University of Technology, Warynskiego 1, 00-645 Warsaw, Poland
[b] Karlsruhe Institute of Technology, Institute of Micro Process Engineering, Hermann von Helmholtz Paltz 1, 76344 Eggenstein, Germany
[c] Siemens AG, Engineering and Consulting, Industrial Park Höchst, B598, 65926 Frankfurt am Main, Germany

ARTICLE INFO

Article history:
Received 26 March 2010
Received in revised form 21 July 2010
Accepted 22 July 2010

Keywords:
Chemical absorption
Mass transfer coefficients
Monoethanolamine
Falling film
Microreactor
Marangoni effect

ABSTRACT

Mass transfer in some gas–liquid systems may be significantly enhanced by the Marangoni effect. In the case of a falling film microreactor (FFMR) for gas–liquid reactions, the question whether the interfacial tension driven cells would develop in the limited space of a microchannel remains unsolved. One way of approaching this problem is to measure the mass transfer rate in a microreactor using a system known to exhibit the Marangoni effect in the macroscale, and to compare this rate with the value determined for the analogous process without this effect. Gas–liquid mass transfer in a FFMR with 29 microchannels (0.6 mm width each) was investigated. CO_2 was absorbed from a CO_2/N_2 gaseous mixture into an aqueous solution of NaOH, and the liquid side mass transfer coefficient as well as the gas side mass transfer coefficient were measured. Then the possibility of appearance of the Marangoni effect was investigated using aqueous monoethanolamine (MEA) solution. The existence of the cellular convection was observed. The enhancement of the overall rate of the mass transfer depends on both gas and amine concentrations.

1. Introduction

The Marangoni effect (cellular convection) occurs in many gas–liquid and liquid–liquid systems and accelerates the mass transfer processes taking place in such systems. Cellular convection is a spontaneous phenomenon occurring in liquids near the interface during heat and/or mass transfer. The system instability is caused by local differences of temperature and/or concentration at the interface which lead to local differences in the value of interfacial tension.

Recently, microstructures are often used to carry out reactions and/or mass transfer processes in two-phase systems. Microstructures ensure significant intensification of mass and heat transfer owing to short diffusion/conduction paths, large concentration/temperature gradients and a high surface to volume ratio. The basic elements of microstructures are microchannels. There are two kinds of microchannels used to contact two different phases: open and closed microchannels [1,2]. Open microchannels have the form of grooves etched or cut in a flat plate, open from one side to ensure contact with the other phase. A typical example of the open microchannel apparatus is the falling film microreactor (FFMR) (see Fig. 1).

In recent years the hydrodynamics of liquid flow in FFMR have been intensively investigated. Yeong et al. [3] measured the film thicknesses using reflection confocal microscopy and observed different cross-sectional profiles of the liquid film surface at various flow rates and in different microchannels. The influence of the contact angle on the liquid profile in microchannels was observed [4,5]. Commenge et al. [6] investigated the gas phase residence time distribution (RTD) in a FFMR, and observed that the formation of recirculation loops at the gas inlet and a jet effect considerably increased the mixing within the gas phase. Mass transfer processes in the FFMR have also been studied. The most popular system used for investigations of the chemical absorption process is the absorption of carbon dioxide in aqueous solutions. Zanfir et al. [7] modelled CO_2 absorption into sodium hydroxide solutions using a two-dimensional model with no adjustable parameters, and compared the results of calculation with experimental data. They concluded, that neither liquid film thickness nor the thickness of the gas film did significantly influence the CO_2 conversion. Numerical simulations of the CO_2 absorption in sodium hydroxide solutions were also performed by Chasanis et al. [8], who used a rigorous 2D model, and by Al-Rawashdeh et al. [4], who used a pseudo-3D model. Both teams compared the results of calculations with available experimental data and claimed reasonably good agreement between them. Chemical reaction with a solid catalyst in the FFMR was also studied. Yeong et al. [9] investigated hydrogenation of nitrobenzene to aniline in ethanol with palladium catalyst in the form of particles or film deposited on the channel

* Corresponding author. Tel.: +48 22 234 63 19; fax: +48 22 825 14 40.
E-mail address: sobieszuk@ichip.pw.edu.pl (P. Sobieszuk).

1385-8947/$ – see front matter © 2010 Elsevier B.V. All rights reserved.
doi:10.1016/j.cej.2010.07.053

Nomenclature

b	stoichiometric coefficient
C_{Ai}	molar concentration of CO_2 at the interface (mole m^{-3})
C_{Ai}^{AV}	average molar concentration of CO_2 at the interface (mole m^{-3})
C_{Ae}^{AV}	average equilibrium concentration (mole m^{-3})
C_{B0}	initial molar concentration of a liquid reagent (mole m^{-3})
d	microchannel width (m)
D_A	diffusivity of CO_2 in water solution (m^2/s)
D_B	diffusivity of the liquid reagent in water solution (m^2/s)
E	enhancement factor
F	interfacial area (m^2)
H	Henry's constant (mole m^{-3} Pa^{-1})
$Ha = (k_2 \cdot C_{B0} \cdot D_A)^{0.5} \cdot k_L^{-1}$	Hatta number
K^*	overall mass transfer coefficient with chemical reaction (m/s)
k_2	reaction rate constant (m^3 $mole^{-1}$ s^{-1})
k_G	gas side mass transfer coefficient (mole m^{-2} s^{-1} Pa^{-1})
k_L	liquid side mass transfer coefficient (m/s)
k_L^*	liquid side mass transfer coefficient for absorption with chemical reaction (m/s)
L	microchannel length (m)
N_A^*	molar mass flux for absorption with chemical reaction (mole m^{-2} s^{-1})
p_A	partial pressure of CO_2 in the gas (Pa)
Q_G	gas flow rate (m^3/s)
Q_L	total liquid flow rate (m^3/s)
R	gas constant (J $mole^{-1}$ K^{-1})
T	temperature (K)

Greek symbols

$\beta = C_{B0} \cdot D_B \cdot (b \cdot C_{Ai}^{AV} \cdot D_A)^{-1}$	concentration ratio

Subscripts

1	inlet
2	outlet
exp	experimental
i	interface
theor	theoretical

wall using different methods. They concluded that the process in a microstructure was feasible, but fast catalyst deactivation was observed.

In the design of a FFMR microreactor for gas–liquid reactions, the question whether the interfacial tension driven cells would develop in the limited space of a microchannel remains unsolved. One way of approaching this problem is to measure the mass transfer rate in a microreactor using a system known to exhibit the Marangoni effect in the macroscale, and to compare this rate with the value determined for the analogous process without this effect. A typical example of a process in which the Marangoni effect is observed is the absorption of carbon dioxide into aqueous solutions of monoethanolamine (MEA) as has been shown for wetted wall columns and packed columns [10,11], whereas the system CO_2–NaOH–H_2O is known not to exhibit this effect.

In this work the CO_2–MEA–H_2O and the CO_2–NaOH–H_2O systems were chosen to elucidate the problem of the appearance of Marangoni type effects in FFMR.

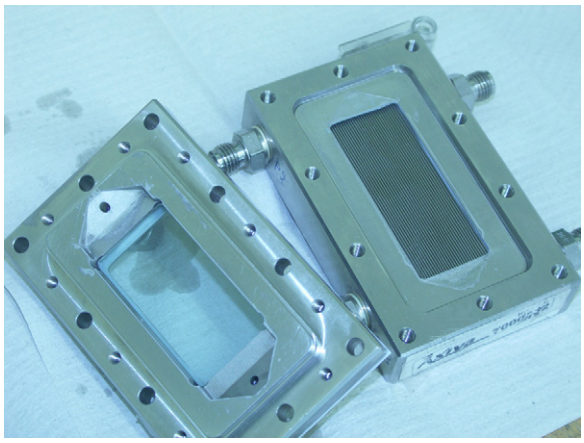

Fig. 1. Falling film microreactor scheme.

2. Experimental technique

The main part of the microreactor is a stainless steel plate with 29 straight, open, vertical, parallel channels 78.3 mm long, 0.3 mm depth and 0.6 width (Fig. 1). The gas phase is flowing concurrently with the liquid between this plate, and a parallel a glass plate 3 mm apart. Nitrogen and carbon dioxide were supplied from cylinders through reducing valves and needle valves. Both gases were mixed before entering the microreactor. The gas flow to the microreactor was measured by an electronic gas flowmeter (made by Brooks). The gas flowmeter measured the volume flow reduced to standard conditions, subsequently corrected for real pressure. Liquid was supplied by a gear pump (Verdergear, made by Verder). At the outlet from FFMR the two phases were separated and the gas phase was directed to the analysis. The inlet and outlet CO_2 concentrations were monitored by the carbon dioxide spectrometric concentration meter SYL&ANT operating in the infrared range. The CO_2 absorption rate was calculated from the concentration changes between gas inlet and outlet. The gas (CO_2/N_2 gaseous mixture) volumetric flow was constant (3.3×10^{-6} m^3/s), the inlet concentration CO_2 was varied between 12% and 97%. The absorption rate was measured for three values of the liquid volumetric flow: 2.55×10^{-7} m^3/s, 3.79×10^{-7} m^3/s and 6.27×10^{-7} m^3/s.

3. Methodology

As explained in Section 1, the problem to solve was whether the Marangoni cells may develop in the limited space of a microchannel. This is important from both theoretical and practical points of view, for the Marangoni effects may strongly enhance the mass transfer rate in the systems exhibiting such effect. One way to solve the problem is to compare the mass transfer rate in a system known to exhibit this effect in macroscale (CO_2–MEA–H_2O) to mass transfer known not to exhibit it (CO_2–NaOH–H_2O).

During the experiments the outlet CO_2 concentration was measured for constant volumetric gas and liquid flow values, constant CO_2 concentration at the gas inlet, and constant NaOH or MEA concentrations at liquid inlet. Then the inlet (p_{A1}) and outlet (p_{A2}) CO_2 partial pressures were calculated. Finally, the carbon dioxide absorption rate (CO_2 molar flux) was found:

$$N_A^* = \frac{1}{RT}\frac{Q_{G1}p_{A1} - Q_{G2}p_{A2}}{F} \quad (1)$$

where F is the interfacial area. The estimation of the interfacial area requires same consideration. In general, interfacial area in the FFMR depends on the shape of the liquid meniscus and the degree of filling of the microchannels. The above parameters depend in turn on

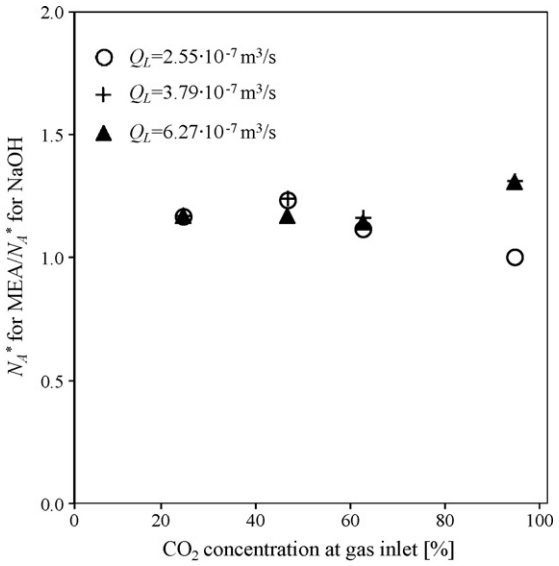

Fig. 2. Comparison of the absorption rates in MEA and NaOH systems (in the same conditions).

the wettability (contact angle) of the channel material by the liquid used, and on the flow rate of the liquid. In our experiments the contact angle is 15–20° (good wettability), and the channels were almost completely filled with the flowing liquid (the liquid film thickness estimated using the Nusselt theory ranges from 0.17 mm to 0.25 mm, but this theory was developed for a flat plate, and underestimates the film thickness in a channel). Under these circumstances the curvature of the meniscus should not increase the interfacial area by more than 12%, as compared to a flat interface. Moreover, possible error in the estimation of the interfacial area would be the same for both physicochemical systems, and therefore should be at least partially compensated or completely cancelled. For these reasons we decided to use the simplest estimate of the interfacial area, namely $F = 29\,L{\cdot}d$.

3.1. Direct comparison of the absorption rate for both systems (CO_2–MEA–H_2O and CO_2–NaOH–H_2O)

The simplest way to check whether the Marangoni effect can occur in the microchannels would be to compare directly the absorption rate for both systems CO_2–MEA-H_2O and CO_2–NaOH–H_2O), under exactly the same conditions (same value of k_G, k_L, same reaction rate, etc.). Such a comparison has been performed for one set of experimental conditions, and the results are shown in Fig. 2. As can be seen, the values of the ratio of the absorption rates measured in both systems are greater than unity, which indicates the appearance of the Marangoni effect. However, this simple method could not be used generally for all the conditions, because of differences in physicochemical properties of both systems (different CO_2 solubility, reaction rate constant, density, viscosity and diffusivity). Moreover, the influence of the Marangoni effect may by diminished by possible influence of the gas phase diffusional resistance (k_G). For these reasons a more elaborate procedure has been used, as explained in the following section.

3.2. CO_2 absorption in 1 M NaOH solution

The physicochemical properties of CO_2–H_2O–NaOH system were widely published. From the available data the following were used: diffusivities [12,13], Henry's constant and second-order reaction rate constant [14].

3.2.1. Liquid side mass transfer coefficient (k_L)

The gas phase with 97% of CO_2 concentration was used. In this case, the gas side mass transfer resistance could be neglected. Thus:

$$p_{A1} = p_{A1i} \qquad p_{A2} = p_{A2i} \tag{2}$$

At the interface the physicochemical equilibrium can be assumed, described by Henry's law:

$$C_{A1i} = H\,p_{A1i} \qquad C_{A2i} = H\,p_{A2i} \tag{3}$$

According to Commenge et al. [6] investigation, for our conditions the equivalent number of CSTR is 8. Therefore, the average concentration of dissolved CO_2 at interface was calculated assuming the piston flow of gas:

$$C_{Ai}^{AV} = \frac{C_{A1i} - C_{A2i}}{\ln C_{A1i}/C_{A2i}} \tag{4}$$

Therefore, the liquid side mass transfer coefficient with chemical reaction was calculated using equation:

$$N_A^* = k_L^*\,C_{Ai}^{AV} \tag{5}$$

The relative increase in absorption rate due to the chemical reaction (enhancement factor) is:

$$E = \frac{k_L^*}{k_L} \tag{6}$$

and the theoretical value of E for the second-order reaction was calculated using the Porter approximation [15]:

$$E = 1 + \beta\left[1 - \exp\left(-\frac{Ha - 1}{\beta}\right)\right] \tag{7}$$

where Ha is the Hatta number for the second-order reaction, $\beta = C_{B0}\cdot D_B(b\cdot C_{Ai}^{AV}\cdot D_A)^{-1}$ is the concentration ratio.

Then the physical mass transfer coefficient (k_L) was calculated from Eqs. (6) and (7) using the trial and error procedure.

3.2.2. Gas side mass transfer coefficient (k_G)

For more diluted gas phase, when the gas phase mass transfer resistance cannot be neglected, the absorption rates on the gas and

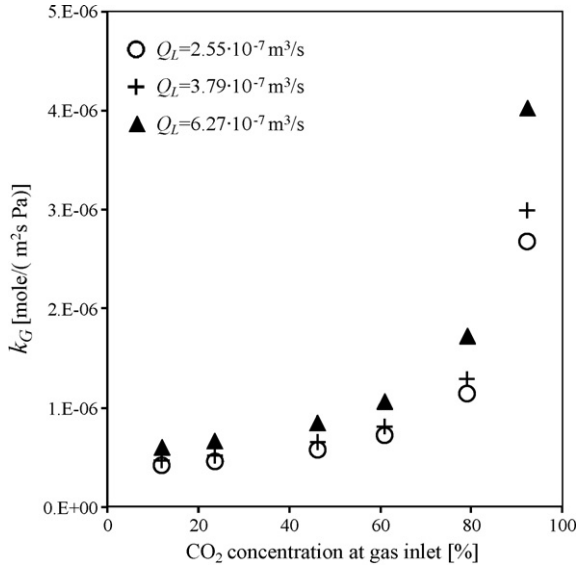

Fig. 3. Gas side mass transfer coefficient.

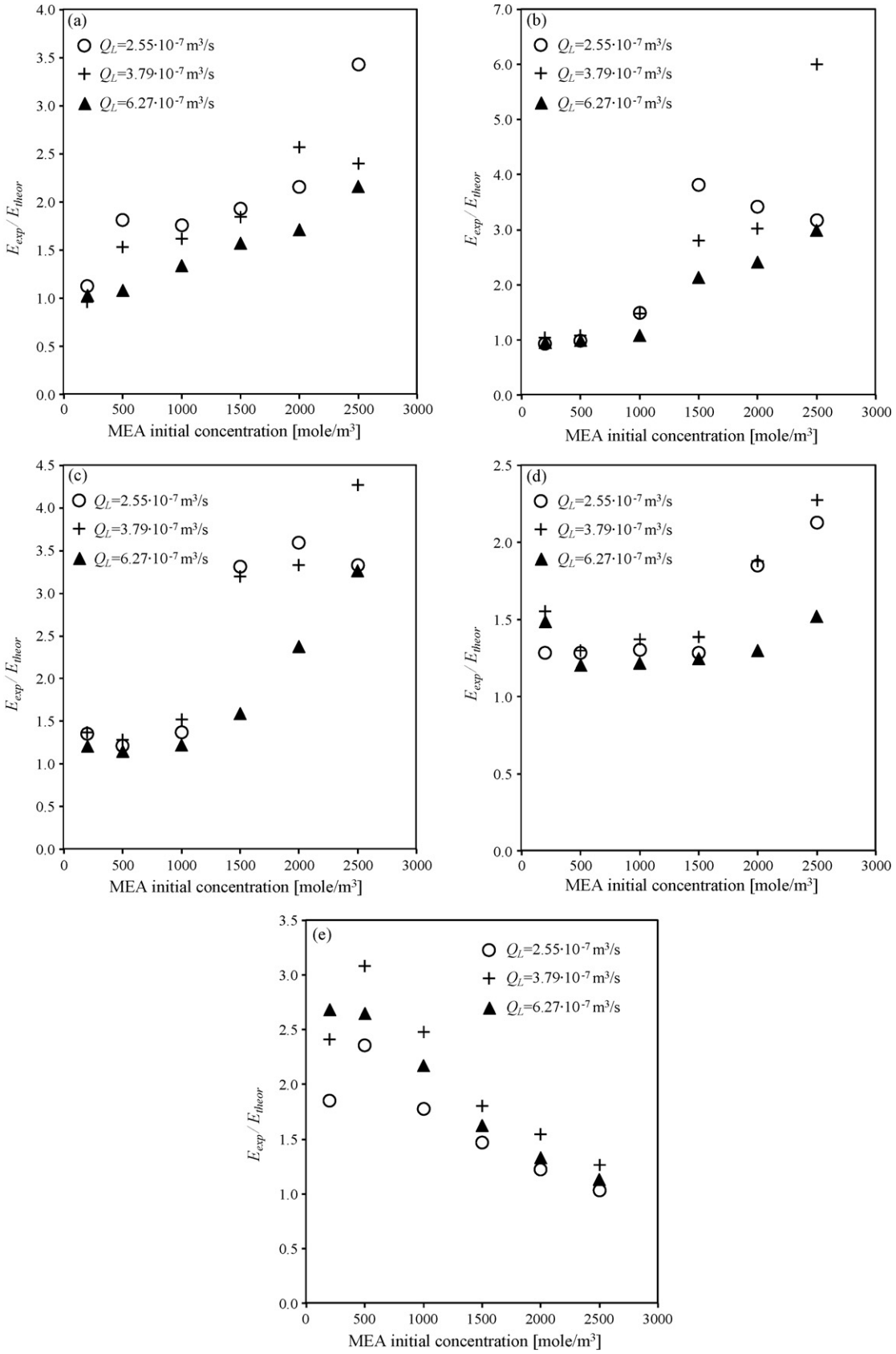

Fig. 4. E_{exp}/E_{theor} factor for (a) 23%, (b) 35%, (c) 45%, (d) 61%, and (e) 93% CO_2 concentrations.

Table 1
Physical liquid side mass transfer coefficient values.

Q_L (m^3/s)	Liquid film thickness (m)	Average liquid velocity (m/s)	k_L (m/s), our experiments	k_L (m/s), Zhang et al. [5]
2.55×10^{-7}	0.17×10^{-3}	0.09	7.22×10^{-5}	10×10^{-5}
3.79×10^{-7}	0.2×10^{-3}	0.11	8.96×10^{-5}	11×10^{-5}
6.27×10^{-7}	0.23×10^{-3}	0.16	12.5×10^{-5}	13×10^{-5}

liquid sides are equal to each other:at the inlet:

$$k_G (p_{A1} - p_{A1i}) = k_L E C_{A1i} \quad (8)$$

similarly at the outlet:

$$k_G (p_{A2} - p_{A2i}) = k_L E C_{A2i} \quad (9)$$

The gas side mass transfer coefficient (k_G) and the enhancement factor (E) values are first assumed. Using suitable value of the physical liquid side mass transfer coefficient (k_L) (measured for 97% concentration of inlet CO_2), combining Eqs. (8) and (9), and using Henry's law (Eq. (3)) the Hatta number (Ha) and concentration ratio (β) can be found. The enhancement factor is again calculated using the Porter approximation (7). The overall mass transfer coefficient with chemical reaction is then found as:

$$K^* = \frac{1}{1/k_L E + H/k_G} \quad (10)$$

and the theoretical absorbed molar flux is determined:

$$N_A^* = K^* C_{Ae}^{AV} \quad (11)$$

where C_{Ae}^{AV} is the average equilibrium concentration:

$$C_{Ae}^{AV} = \frac{p_{A1} H - p_{A2} H}{\ln[(p_{A1} H)/(p_{A2} H)]} \quad (12)$$

The theoretical absorbed molar flux (11) was compared with the experimental absorbed molar flux (1) and the trial and error procedure was used to find the k_G value. In this way the gas side mass transfer coefficient values were found.

3.3. CO_2 absorption in MEA solutions

The physicochemical properties of CO_2–MEA–H_2O system can be found in the literature. From the available data the following were used: diffusivities [16], Henry's constant [17] and second-order reaction rate constant [17]. The molar flux of absorbed CO_2 at inlet and outlet, respectively, can be written as:

$$N_A^* = k_G \left(p_{A1} - \frac{C_{A1i}}{H} \right) \quad (13)$$

$$N_A^* = k_G \left(p_{A2} - \frac{C_{A2i}}{H} \right) \quad (14)$$

From Eqs. (13), (14) and (4) the average molar concentration of CO_2 at the interface C_{Ai}^{AV} was obtained. This allows to calculate (from Eq. (5)) the experimental values of the liquid side mass transfer coefficient for the absorption with chemical reaction. Finally, the experimental enhancement factor (E_{exp}) is calculated using (Eq. (6)). On the other hand the theoretical enhancement factor value (E_{theor}) is calculated for second-order reaction using approximation (Eq. (7)). The E_{exp}/E_{theor} ratio is a measure of the influence of the cellular convection on the overall rate of mass transfer.

4. Results and discussion

In the first step, the physical liquid side mass transfer coefficient was determined using the 97% CO_2 absorption in 1 M NaOH solution process. Table 1 shows the k_L values for three liquid volumetric flow rates. The k_L values increase with increasing Q_L and are close to those obtained by Zhang et al. [5].

In the second step, using the k_L values measured for CO_2 absorption in 1 M NaOH solution, the gas side mass transfer coefficient values were obtained. These measurements were carried out for six different concentrations of CO_2 in the gas phase (in the range 12–93%). Fig. 3 shows the k_G values. As can be seen, the k_G values increase with increasing CO_2 concentration, exhibiting a very significant increase for 93%. This is in agreement with the theory. For a pure gas k_G approaches infinity. Slight increase of k_G values with Q_L was observed.

In third step absorption of CO_2 in MEA solutions was studied. Several CO_2 concentration values in inlet gas (23%, 35%, 45%, 61% and 93%) and several MEA concentrations in liquid (0.2 M, 0.5 M, 1.0 M, 1.5 M, 2.0 M and 2.5 M) were used. The liquid and gas side mass transfer coefficients measured previously using CO_2–H_2O–NaOH system (steps 1 and 2, respectively) were used as explained above. Fig. 4a–e shows the dependence E_{exp}/E_{theor} ratio for different initial MEA concentrations. As can be seen, there is significant enhancement of the absorption rate caused by the Marangoni effect. This means that convection cells can develop even in the limited space of the microchannel. For lower CO_2 concentration this enhancement increases with increasing amine concentrations as expected. For MEA concentrations in the range 2–2.5 M a 3- to 6-fold increase in the absorption rate is observed. More complicated phenomena are observed for higher CO_2 concentrations. For CO_2 concentrations higher than 50% a significant increase in the absorption rate is observed for very low amine concentration. Then the effect passes a minimum, and increases again for high MEA concentrations. The reasons for such behavior are not clear and require further investigation. Attempts to compare the results obtained in this work with the existing correlations [10,18] did not give univocal conclusions. Generally, our results show weaker effect of interfacial phenomena than predicted by Buzek's [18] correlation. This may mean that the cellular convection on our case has been partially hindered by the limited size of the microchannel. However, all the above-mentioned correlations predict monotonic dependence of the Marangoni effect on both amine and gas concentrations, whereas our results indicate more complex behavior. Clearly, the quantitative description of the effect, as well as prediction of the lower limit of the size of the channel still permitting the effect to develop, require more experimental data and should be further investigated. It should also be borne in mind, that the results may be influenced by the deviations from the piston flow both in the gas and in the liquid phase (Taylor dispersion). This problem shall also be further investigated.

5. Conclusions

The appearance of the Marangoni effect in a falling film microreactor with 0.3 mm × 0.6 mm microchannels has been experimentally demonstrated. The enhancement of the mass transfer rate in the CO_2–monoethanolamine–H_2O system has been measured. Attempts to compare the results obtained in this work with the existing correlations did not give univocal conclusions. The effect measured in a microreactor seems to be weaker than that measured in macrosystems, which may mean that the cellular

convection on our case has been partially hindered by the limited size of the microchannel. However, the quantitative description of the effect requires more experimental data and should be further investigated.

References

[1] R. Pohorecki, P. Sobieszuk, K. Kula, W. Moniuk, M. Zieliński, P. Cygański, P. Gawiński, Hydrodynamic regimes of gas–liquid flow in a microreactor channel, Chem. Eng. J. 135S (2008) S185–S190.

[2] P. Sobieszuk, P. Cygański, R. Pohorecki, Volumetric mass transfer coefficient in a gas–liquid microreactor, Chem. Proc. Eng. 29 (2008) 651–661.

[3] K.K. Yeong, A. Gavriilidis, R. Zapf, H.J. Kost, V. Hessel, A. Boyde, Characterization of liquid film in a microstructured falling film reactor using laser scanning confocal microscopy, Exp. Therm. Fluid Sci. 30 (2006) 463–472.

[4] M. Al-Rawashdeh, V. Hessel, P. Löb, K. Mevissen, F. Schönfeld, Pseudo 3-D simulation of a falling film microreactor based on realistic channel and film profiles, Chem. Eng. Sci. 63 (2008) 5149–5159.

[5] H. Zhang, G. Chen, J. Yue, Q. Yuan, Hydrodynamics and mass transfer of gas–liquid flow in a falling film microreactor, AIChE J. 55 (2009) 1110–1120.

[6] J.M. Commenge, T. Obein, G. Genin, X. Framboisier, S. Rode, V. Schanen, P. Pitiot, M. Matlosz, Gas-phase residence time distribution in a falling-film microreactor, Chem. Eng. Sci. 61 (2006) 597–604.

[7] M. Zanfir, A. Gavriilidis, Ch. Wille, V. Hessel, Carbon dioxide absorption in a falling film microstructured reactor: experiments and modeling, Ind. Eng. Chem. Res. 44 (2005) 1742–1751.

[8] P. Chasanis, A. Lautenschleger, E.Y. Kenig, Numerical investigation of carbon dioxide in a falling-film micro-reactor, Chem. Eng. Sci. 65 (2010) 1125–1133.

[9] K.K. Yeong, A. Gavriilidis, R. Zapf, V. Hessel, Catalyst preparation and deactivation issues for nitrobenzene hydrogenation in a microstructured falling film reactor, Catal. Today 81 (2003) 641–651.

[10] K. Warmuziński, J. Buzek, J. Podkański, Marangoni instability during absorption accompanied by chemical reaction, Chem. Eng. J. 58 (1995) 151–160.

[11] J. Buzek, J. Podkański, K. Warmuziński, The enhancement of the rate of absorption of CO_2 in amine solutions due to the Marangoni effect, Energy Convers. Manage. 38 (1997) S69–S74.

[12] G.F. Versteeg, W.P.M. van Swaaij, Solubility and diffusivity of acid gases (CO_2, N_2O) in aqueous alkanolamine solutions, J. Chem. Eng. Data 33 (1988) 29–34.

[13] W. Moniuk, R. Pohorecki, Viscosity and density of sodium and potassium alkaline solutions, Hung. J. Ind. Chem. 19 (1991) 175–178.

[14] R. Pohorecki, W. Moniuk, Kinetics of reaction between carbon dioxide and hydroxyl ions in aqueous electrolyte solutions, Chem. Eng. Sci. 43 (1988) 1677–1684.

[15] K.E. Porter, The effect of contact-time distribution on gas absorption with chemical reaction, Trans. Inst. Chem. Eng. 44 (1966) T25–T36.

[16] H. Hikita, H. Ishikawa, K. Uku, T. Murakami, Diffusivities of mono-, di-, and triethanolamines in aqueous solutions, J. Chem. Eng. Data 25 (1980) 324–325.

[17] P.V. Danckwerts, K.M. McNeil, The absorption of carbon dioxide into aqueous amine solutions and the effects of catalysis, Trans. Inst. Chem. Eng. 45 (1967) T32–T49.

[18] J. Buzek, Cellular convection during absorption with chemical reaction, Zesz. Nauk. Politech. Śląsk. Gliwice 90 (1979) 93–94 (in Polish).